Cancer Research

The Biodistribution and Immune Suppressive Effects of Breast Cancer–Derived Exosomes

Shu Wen Wen[1], Jaclyn Sceneay[1], Luize Goncalves Lima[1], Christina S.F. Wong[1], Melanie Becker[1], Sophie Krumeich[1], Richard J. Lobb[1], Vanessa Castillo[1], Ke Ni Wong[1], Sarah Ellis[2], Belinda S. Parker[3], and Andreas Möller[1,4]

Abstract

Small membranous secretions from tumor cells, termed exosomes, contribute significantly to intercellular communication and subsequent reprogramming of the tumor microenvironment. Here, we use optical imaging to determine that exogenously administered fluorescently labeled exosomes derived from highly metastatic murine breast cancer cells distributed predominantly to the lung of syngeneic mice, a frequent site of breast cancer metastasis. At the sites of accumulation, exosomes were taken up by $CD45^+$ bone marrow–derived cells. Subsequent long-term conditioning of naïve mice with exosomes from highly metastatic breast cancer cells revealed the accumulation of myeloid-derived suppressor cells in the lung and liver. This favorable immune suppressive microenvironment was capable of promoting metastatic colonization in the lung and liver, an effect not observed from exosomes derived from nonmetastatic cells and liposome control vesicles. Furthermore, we determined that breast cancer exosomes directly suppressed T-cell proliferation and inhibited NK cell cytotoxicity, and hence likely suppressed the anticancer immune response in premetastatic organs. Together, our findings provide novel insight into the tissue-specific outcomes of breast cancer–derived exosome accumulation and their contribution to immune suppression and promotion of metastases. *Cancer Res; 76(23); 6816–27. ©2016 AACR.*

Introduction

Despite improvements in screening and therapy, breast cancer remains the most common type of cancer and the second-leading cause of cancer-related death in women (1). Currently, it is not possible to accurately predict the risk of developing metastatic disease or the response of patients to treatment, and this is reflected in up to 20% of patients who ultimately die of metastatic breast cancer (1, 2). The cross-talk between cancer cells and their surrounding stroma is essential in regulating tumor progression and systemic spread (3). While tumor cells are classically described to communicate via direct cell-to-cell contact and the secretion of soluble factors, such as cytokines and growth factors (4), alternative mechanisms have recently been described. One of these involves small membranous particles secreted from cancer cells, termed exosomes, which contribute significantly to the intercellular communication and subsequent reprogramming of the tumor microenvironment (5, 6). Exosomes are extracellular vesicles of endocytic origin with a size of 30 to 120 nm that are released under both physiological and pathological conditions (5). The content of exosomes reflects the cell of origin and includes lipids, proteins, messenger RNA and microRNA, which are transferred from donor to target cells. In target cells, the content is thought to induce functional changes capable of promoting metastatic progression, including contribution to premetastatic niche formation (7–10). Therefore, cancer-secreted exosomes and their molecular contents have received much attention as potential biomarkers and therapeutic targets for cancer (5, 6, 11).

Reduced immune surveillance is a key mechanism through which primary tumors create permissive environments in secondary organs that favor the development of metastasis (premetastatic niche formation; refs. 12–14). Studies have reported that tumor-derived exosomes can have detrimental effects on the immune system by suppressing specific T-cell immunity and skew innate immune cells toward a protumor phenotype (15–17). Most recently, pancreatic cancer exosomes were shown to increase liver metastatic burden by transferring macrophage migration inhibitory factor (MIF) to liver macrophages and by recruiting immune cells to initiate premetastatic niche formation in the liver (12). However, it remains to be determined whether exosomes can induce premetastatic niches in other types of cancers, such as breast cancer. Moreover, it remains unclear which immune cell lineage in specific organs is largely responsible for the uptake of circulating tumor-secreted exosomes and its subsequent impact on anticancer immune responses during metastasis.

[1]Tumor Microenvironment Laboratory, QIMR Berghofer Medical Research Institute, Herston, Queensland, Australia. [2]Peter MacCallum Cancer Centre, East Melbourne, and Sir Peter MacCallum Department of Histology, University of Melbourne, Parkville, Australia. [3]Department of Biochemistry and Genetics, La Trobe Institute for Molecular Science, La Trobe University, Melbourne, Victoria, Australia. [4]School of Medicine, University of Queensland, Brisbane, Queensland, Australia.

Note: Supplementary data for this article are available at Cancer Research Online (http://cancerres.aacrjournals.org/).

Current address for Jaclyn Sceneay: Hematology Department, Brigham and Women's Hospital, Harvard Medical School, Boston, Massachusetts.

Corresponding Author: Andreas Möller, QIMR Berghofer Medical Research Institute, 300 Herston Road, Herston, Australia, 4006. Phone: 61738453950; Fax: 61738453950; E-mail: andreas.moller@qimrberghofer.edu.au

doi: 10.1158/0008-5472.CAN-16-0868

Here, we report a detailed analysis of the tissue distribution of intravenously injected exosomes from breast cancer cells with differing metastatic potential, their uptake by various immune cell lineages, and the immunosuppressive outcomes of exosome accumulation in premetastatic organs.

Materials and Methods

Mice

Female C57BL/6 and BALB/c mice were purchased from the Walter and Eliza Hall Institute (Australia) and used at 8 to 12 weeks of age. All animal procedures were conducted in accordance with Australian National Health and Medical Research regulations on the use and care of experimental animals, and approved by the QIMR Berghofer Medical Research Institute Animal Ethics Committee (P1499).

Cell culture

The murine C57BL/6 EO771 and isogenic BALB/c 4T1 and 67NR cells were generated and maintained as previously described (18–22). No authentication protocol exists for these cell lines according to our knowledge. The cells tested negative for *mycoplasma* contamination and this testing was conducted every 3 months and after taking cells into culture.

Exosome isolation

Exosomes from EO771 cells were purified from cell culture supernatants by a combination of ultracentrifugation, ultrafiltration, and size exclusion purification as previously described (23). Briefly, cultured cells at 60% to 70% confluence were washed three times in PBS and grown for 24 hours in serum-free media. Conditioned media were collected, with dead cells and large debris removed by centrifugation (500 × *g*; 10 minutes), followed by filtration (0.22 μm). The resulting cell-free medium was concentrated by ultrafiltration using the Centricon Plus-70 Centrifugal Filter (100 kDa; Merck Millipore) at 3,500 × *g*, 4°C.

Purification of exosomes from concentrated media was performed by overlaying on qEV size exclusion columns (Izon Science Ltd) followed by sample concentration in Amicon Ultra-4 10-kDa nominal molecular weight centrifugal filter units (Merck Millipore) to a final volume of 200 μL for further analysis (23).

Isolation of exosomes from 4T1 and 67NR cells was carried out as previously described (12, 15, 24). Briefly, cell lines were grown in FBS-supplemented culture media that was depleted of exosomes. Supernatant fractions were collected from 48-hour cell cultures, followed by centrifugation (500 × *g*; 10 minutes) and filtration (0.22 μm) to remove dead cells and large debris. Exosomes were collected, washed in PBS, and pelleted by ultracentrifugation at 100,000 × g for 90 minutes at 4°C.

Electron microscopy

Electron microscopy imaging was performed as described (25) with modifications. Briefly, purified exosomes were fixed with paraformaldehyde and transferred to Formvar-carbon–coated electron microscopy grids. Grids were transferred to 1% (v/v) glutaraldehyde for 5 minutes, followed by eight washes with water. For contrast, grids were negatively stained with 1% (w/v) uranyl-oxalate solution, pH 7 for 5 minutes before transferring to methyl-cellulose-UA for 10 minutes. Excess fluid was removed and exosomes were imaged in a JEOL 1011 transmission electron microscope at 60 kV.

Western blotting

Exosome preparations were solubilized with Laemmli sample buffer, protein quantified using a standard Bradford Assay, and analyzed by Western blotting as previously described (20). The membrane was probed with the following primary antibodies: mouse anti-flotillin-1 (610821; BD Biosciences), goat anti-tsg101 (M-19sc-6037; Santa Cruz Biotechnology), rabbit anti-CD9 (ab92726; Abcam), mouse anti-HSP70 (610608; BD Biosciences), and rabbit anti-GM130 (ab52649; Abcam). Samples were further incubated with the appropriate secondary antibodies: goat anti-rabbit HRP (1858415; Pierce), goat anti-mouse HRP (1858413; Pierce), or rabbit anti-goat HRP (A5420; Sigma-Aldrich).

Size distribution analysis by tunable resistive pulse sensor

The quantification and size distribution analysis of exosomes was performed using the Izon qNano system by tunable resistive pulse sensor (TRPS) technology (Izon Science Ltd) with the NP100 nanopore and 70-nm calibration beads (CPS70) as previously reported (26, 27).

In vivo imaging of fluorescently labeled exosomes and tracking

Purified exosomes were fluorescently labeled using Vybrant DiD (Life Technologies) according to the manufacturer's instructions with modifications. Briefly, exosomes and liposomes were incubated for 10 minutes with DiD (1:1000 dilution in PBS). Excess dye was removed by washing in 20 mL of PBS at 100,000 × g (90 minutes) to receive the final DiD-stained exosome preparation. DiD-labeled exosomes derived from EO771, 4T1, or 67NR cells were injected intravenously either into syngeneic C57BL/6 or BALB/C mice (20 μg of exosomes/mouse). At 4, 24, and 48 hours after injection, various tissues were harvested (lung, spleen, kidney, liver, heart, and bone marrow) for *in vivo* and *ex vivo* imaging. The intensity of fluorescence was quantified using the IVIS Spectrum and Living Image Software (PerkinElmer) to assess tissue distribution of DiD-labeled exosomes. Additionally, immune populations in the lung, spleen, and bone marrow that had taken up DiD-labeled exosomes were assessed using flow cytometry.

Premetastatic niche formation and experimental metastasis studies

To initiate premetastatic niche formation, C57BL/6 or BALB/c mice were injected intravenously (tail vein) with either 10 μg (EO771) or 5 μg (4T1 and 67NR) exosomes, every 3 days for 30 days, or a once-off injection of 50 μg of EO771 exosomes. EO771 exosomes (1 μg) is equivalent to approximately 7.9×10^9 particles, and 1 μg of 4T1 and 67NR exosomes is equivalent to approximately 5.8×10^9 particles as determined by the TRPS and Bradford assays. After exosome injection, lungs, spleen, and bone marrow were harvested, and immune cell composition was assessed using flow cytometry. Alternatively, after exosome conditioning (exosomes injected every 3 days for 30 days), mice received 1×10^5 EO771 cells via the tail vein (experimental metastasis model) and metastatic burden in the lung was assessed 21 days later, or 2.5×10^5 4T1-luciferase cells via the tail vein, and metastatic burden in the lung and liver assessed 14 days later. Control mice received an equivalent particle number of synthetic unilamellar 100-nm liposomes (Encapsula Nanoscience) as determined using TRPS or PBS.

Flow-cytometry analysis

Flow cytometry was carried out on single-cell suspensions of whole lung, spleen, bone marrow, and/or liver tissue. A standard protocol was used to prepare single-cell suspensions: (i) lungs were minced and then digested with 0.2 mg/mL collagenase type IV (Worthington Biochemical Corp.) for 20 minutes at 37 °C; (ii) spleen was minced to release splenocytes; (iii) liver was minced, digested with 0.2 mg/mL collagenase type IV for 30 minutes at 37°C, and hepatocytes removed by Percoll gradient; (iv) bone marrow cells were flushed from both the tibia and femur. All cell preparations were passed through a 40-μm filter to obtain single-cell suspensions and treated with Ammonium chloride red cell-lysis buffer. Samples were stained with the appropriate antibodies, together with Fc receptor blocking using anti-CD16/32 before resuspension in FACS buffer containing 2% FBS and viability dye. 7-Aminoactinomycin D (7-AAD) was used as the viability dye, or Zombie Yellow Fixable Viability Kit (BioLegend) for fixed samples. DiD-labeled exosome-positive cells were detected using red laser excitation and 640-nm emission. Flow-cytometric acquisition was completed using a LSR-Fortessa (BD Biosciences), and analysis was performed using FlowJo (Tree Star).

T-cell proliferation assay

$CD4^+/CD11c^-$ and $CD8^+/CD11c^-$ cells were sorted using fluorescence-activated cell sorting (FACS) from whole spleen tissue from C57BL/6 mice. A standard T-cell proliferation assay using 5-(and -6)-carboxyfluorescein diacetate succinimidyl ester (CFSE; 5 μmol/L) was performed with modifications (28). Briefly, CFSE-labeled $CD4^+/CD11c^-$ and $CD8^+/CD11c^-$ T cells were cocultured with irradiated splenocytes, monoclonal anti-CD3 (0.5 μg/mL) for T-cell stimulation and with varying protein amounts (μg) of EO771-derived exosomes for 72 hours prior to flow-cytometry analysis. Control $CD4^+/CD11c^-$ and $CD8^+/CD11c^-$ T cells received the same volume of PBS or an equivalent particle number of synthetic unilamellar 100-nm liposomes (Encapsula Nanoscience) as determined using TRPS.

51Cr release cytotoxicity assay

$NK1.1^+/CD3^-$ cells were sorted using FACS from whole spleen tissue from C57BL/6 mice and cultured as previously described (29). NK cells were expanded in culture media containing IL2 (1,000 units/mL) for 5 days. ^{51}Cr-labeled YAC-1 target cells were used in a standard 5-hour NK cell cytotoxicity assay at different target (YAC-1 cells) to effector cell (NK cells) ratios and performed as previously described (29, 30). $NK1.1^+/CD3^-$ cells were treated with varying protein amounts (μg) of EO771-derived exosomes for 3 hours prior to incubation with target YAC-1 cells. Control $NK1.1^+/CD3^-$ cells received the same volume of PBS.

Statistical analysis

Quantitative data are presented as mean ± SEM. Non-parametric data were analyzed by two-tailed Mann–Whitney *U* tests. Parametric data were analyzed using ANOVA with *post hoc* comparison (Tukey method). The Holm–Sidak multiple testing correction method was used. Adjusted $P < 0.05$ was considered statistically significant.

Results

Spatial and temporal distribution of breast cancer–derived exosomes

We first characterized and confirmed exosome isolation from the conditioned medium of C57BL/6 EO771 and BALB/c 4T1-syngeneic murine breast cancer cell lines (Supplementary Fig. S1). The morphology of isolated exosomes, as assessed by transmission electron microscopy, showed the typically associated double-layered spherical structure (Supplementary Fig. S1A). Additionally, exosomes were of the correct size and exhibited various marker proteins (Supplementary Fig. S1A–S1C; ref. 6). Particles were positive for exosomal core protein markers, including CD9, HSP70, and TSG101 (Supplementary Fig. S1B, E lanes), and negative for the cis-Golgi marker GM130, which was only present in cell lysates (Supplementary Fig. S1B, C lanes). Using TRPS technology, we determined the mode size of exosomes to be 86 nm and 80 nm for EO771 and 4T1 cells, respectively (Supplementary Fig. S1C). Furthermore, EO771 (1.14×10^{12} particles/ml) and 4T1 cells (1.07×10^{12} particles/ml) displayed similar levels of exosome secretion (Supplementary Fig. S1D).

To elucidate the role of breast cancer exosomes in intercellular communication and its target effects, it is of utmost importance to first determine the *in vivo* fate of exosomes. Here, we studied the biodistribution of breast cancer exosomes in syngeneic mice after systemic delivery. As a majority of mortalities from breast cancer are due to metastatic disease (1, 2) and high exosome abundance in patient plasma correlates to tumor grade and poor patient outcomes (15, 31, 32), we examined the tissue distribution of exosomes derived from highly metastatic EO771 and 4T1 cells, and compared it to nonmetastatic 67NR cells to assess if differences in metastatic potential between isogenic breast cancer cells can influence the uptake and tissue biodistribution of tumor exosomes. 67NR cells produce approximately 13-fold fewer exosomes than 4T1 cells (Supplementary Fig. S1E). EO771-, 4T1-, and 67NR-derived exosomes were labeled with a lipid-associating fluorescent dye, DiD, and administered intravenously. Exosome biodistribution in various organs (lung, spleen, kidney, liver, heart, and bone marrow) was assessed 24 hours after injection using *in vivo* and *ex vivo* imaging and compared with liposome controls.

In vivo and *ex vivo* fluorescence quantification determined significant accumulation of EO771-derived exosomes in the lung (13-fold signal increase), liver, and spleen (2.5-fold signal increase in both tissues) within 24 hours after injection (Fig. 1A; and Supplementary Fig. S2). By 48 hours, this signal was significantly decreased (Supplementary Fig. S2). For this reason, we chose to use the 24-hour time point for further analysis. Accumulation of EO771 exosomes in the bone marrow was detected in some long bones of individual mice, but overall fluorescence quantification showed that this was not statistically significant when compared with liposome-treated controls (Fig. 1A).

Similarly, 4T1- and 67NR-derived exosomes accumulated primarily in the lung (2.8-fold and 5.5-fold signal increase, respectively) within 24 hours after injection compared with liposome-injected control animals (Fig. 1B), further suggesting the retention of tumor exosomes in specific tissues. However, in contrast to 4T1, exosomes from nonmetastatic 67NR cells also accumulated significantly in the liver (3-fold increase; Fig. 1B). Additionally, despite injecting the same number of DiD-labeled

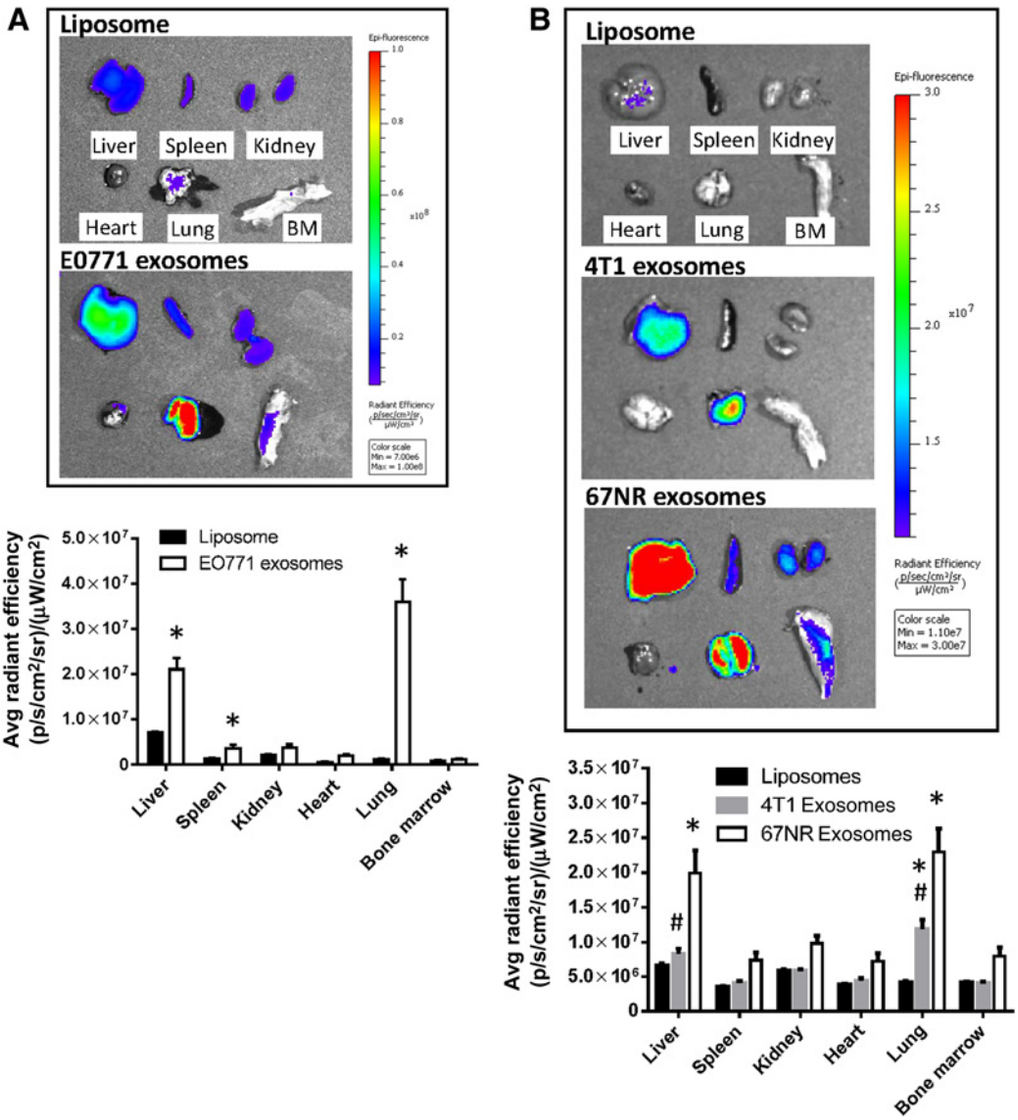

Figure 1.

Visualization and *ex vivo* tracking of breast cancer exosomes. Animals received a single intravenous injection of DiD-labeled EO771-, 4T1-, or 67NR-derived exosomes (20 μg; 1.6×10^{11} EO771 exosomes and 1.2×10^{11} 4T1/67NR exosomes). DiD-labeled liposomes served as control. Tissues were harvested 24 hours after intravenous injection, and fluorescence was visualized and quantified using the IVIS Spectrum (PerkinElmer). Representative *ex vivo* images and quantification (average radiant efficiency) of DiD-labeled EO771 exosomes (**A**) and DiD-labeled 4T1 and 67NR exosomes (**B**). Results are presented as mean ± SEM ($n = 5$–7/group) as analyzed by ANOVA; *, $P < 0.01$ compared with liposome control; #, $P < 0.01$ compared with 67NR DiD exosomes.

vesicles, both the liver and lung showed higher retention of 67NR exosomes after 24 hours compared with 4T1 exosomes (Fig. 1B). Overall, this suggests metastatic potential and/or cellular origin has an important influence on the biodistribution pattern of exosomes.

Breast cancer–derived exosomes are internalized and affect immune cell populations

Next, to determine the cell lineages that were taking up the fluorescent-labeled EO771 exosomes, $CD45^+$ cells in the lung and spleen were assessed as these organs showed significant exosome accumulation (Fig. 2). $CD45^+/DiD^+$ cells represented 14.2% ± 0.44 and 3.2% ± 0.15% of $CD45^+$ cells in the lung and spleen, respectively (Fig. 2A). Despite no major EO771 exosome retention in the bone marrow (Fig. 1A, *ex vivo* fluorescence quantification), more in-depth flow cytometry analysis demonstrated 2.6% ± 0.28% of bone marrow $CD45^+$ cells to have taken up exosomes (Fig. 2A). Within each $CD45^+$ cell subpopulation, $CD11b^+$ myeloid cells (Fig. 2B), dendritic cells (DC; $CD11C^+/MHCII^+$; Fig. 2C), and macrophages (mø; $CD11b^+/F4/80^+$; Fig. 2D) showed high uptake of EO771-derived exosomes, ranging approximately between 40%–60% uptake in the lung and 20%–30% uptake in the spleen. In contrast, EO771 exosome uptake was much lower by NK cells ($NK1.1^+/CD3^-$; Fig. 2E), CD4 T cells

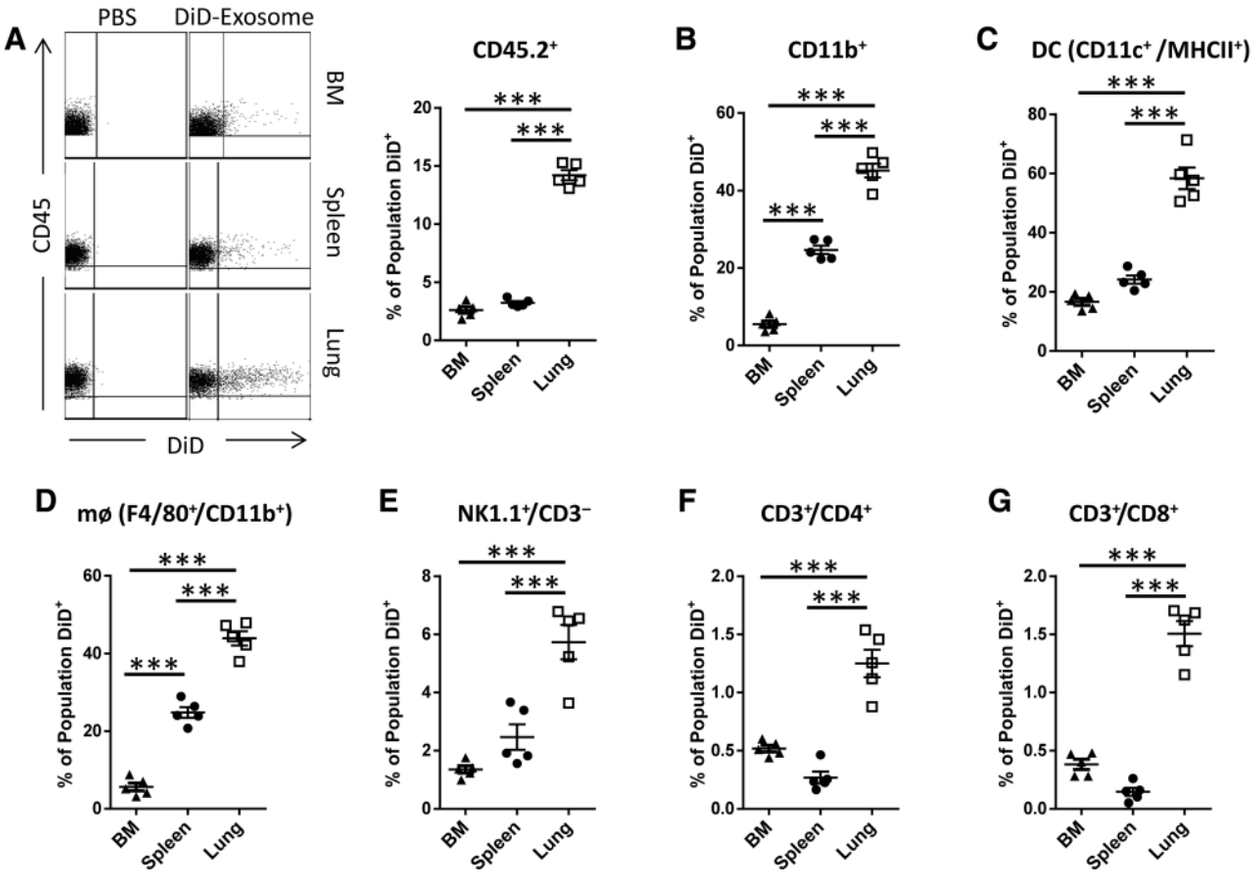

Figure 2.

Uptake of EO771 breast cancer exosomes by immune cell lineages. C57BL/6 mice received a single intravenous injection of DiD-labeled EO771-derived exosomes (20 μg; 1.6×10^{11} particles) or PBS (control). Exosome uptake by immune populations in the bone marrow (BM), spleen, and lung was analyzed 24 hours later by flow cytometry. **A,** Representative flow cytometric plots (left) and quantification (right) of distinct DiD^+ population within $CD45^+$ cells. **B–G,** Frequency of the DiD^+ subpopulation within myeloid cells ($CD11b^+$; **B**), DCs ($CD11C^+/MHCII^+$; **C**), macrophages (mø; $CD11b^+/F4/80^+$; **D**), NK cells ($NK1.1^+/CD3^-$; **E**), CD4 T cells ($CD3^+/CD4^+$; **F**), and CD8 T cells ($CD3^+/CD8^+$; **G**). Results are presented as mean ± SEM ($n = 5$/group) as analyzed by ANOVA; ***, $P < 0.001$.

($CD3^+/CD4^+$; Fig. 2F), and CD8 T cells ($CD3^+/CD8^+$; Fig. 2G). In line with the degree of exosome uptake by $CD45^+$ cells, EO771 exosome uptake by various target immune subpopulations was highest in the lung, followed by the spleen, with least uptake observed in the bone marrow.

A similar uptake pattern by immune populations was observed for fluorescent-labeled exosomes derived from metastatic 4T1 and nonmetastatic 67NR cells (Supplementary Fig. S3). $CD45^+$ cells in the lung displayed highest uptake of exosomes from both tumor cell lines when compared with the spleen and bone marrow, along with minimal uptake of liposome control vesicles (Supplementary Fig. S3A). The uptake of 67NR exosomes by $CD11b^+$ cells, $CD11b^+/Gr1^+$ cells, DCs, and macrophages was significantly higher compared with 4T1 exosomes in most organs assessed (Supplementary Fig. S3B–S3E). Similar to EO771 exosomes, there was minimal uptake of both 4T1- and 67NR-derived exosomes by CD8 and CD4 T cells (Supplementary Fig. S3F–S3G).

To assess the functional consequences of breast cancer exosome accumulation on $CD45^+$ cell lineages, we first determined the composition of immune cells after an acute intravenous injection of unlabeled EO771 exosomes. There were no significant changes in the frequency of myeloid cells, DCs, macrophages, or NK cells in the lung 24 hours after one injection of EO771 exosomes (50 μg/mouse; Supplementary Fig. S4A–S4D). However, a significant decrease in the frequency of CD4 and CD8 T cells (Supplementary Fig. S4E-F) compared with liposome-injected control animals was observed. This suggests the acute ability of breast cancer exosomes to alter immune microenvironments at distant organs. In organs such as the bone marrow, that showed minimal, nonsignificant accumulation of EO771 exosomes, no change in immune cell composition was observed (Supplementary Fig. S5).

To further examine the role of breast cancer–derived exosomes in conditioning the lung to potentially create a premetastatic niche, EO771-derived exosomes were injected intravenously into mice every 3 days for 30 days (Fig. 3A). Subsequent characterization of infiltrating immune cells in the lung confirmed significant changes in immune composition. EO771-derived exosomes increased overall $CD45^+$ cell abundance in the lung, suggesting higher accumulation or infiltration of immune cells to the tissue environment (Supplementary Fig. S6A). While absolute numbers of CD8 T cells, macrophages, and NK cells were unchanged, the

frequency of these cells was altered (Fig. 3; Supplementary Fig. S6B–S6E). Specifically, EO771-derived exosomes reduced the frequency of CD8 T cells and NK cells, but increased macrophage frequency compared with liposome control animals (Fig. 3B and 3E–F). Despite no change in overall CD4 T-cell frequency (Fig. 3B), exosome conditioning did decrease the subpopulation of naïve CD4 T cells ($CD44^{low}/CD62L^{high}$) while increasing frequency of effector memory CD4 T cells ($CD44^{high}/CD62L^{low}$; Fig. 3C). Importantly, EO771 exosomes increased both the frequency and absolute numbers of $CD11b^{+}/Ly6C^{med}$ granulocytic myeloid-derived suppressor cells (gMDSC), but not $CD11b^{+}/Ly6C^{high}$ monocytic MDSCs (mMDSC; Fig. 3G, and Supplementary Fig. S6F). The MDSC population has been previously shown to create premetastatic niches permissive to metastatic colonization (30) and suppress T-cell activity (33, 34). Indeed, we showed that increased gMDSCs accumulation in the lung correlated with a decreased ratio of $CD8^{+}$ T-cell numbers to gMDSCs (Supplementary Fig. S6G). These data indicate that breast cancer exosomes may be capable of initiating premetastatic niche development by skewing the lung microenvironment to an immunosuppressive state. Assessment of the spleen did not indicate significant changes in immune composition after exosome conditioning, except for a slight decrease in NK cell frequency (Supplementary Fig. S7).

We next determined if the overall immunosuppressive environment created in the lung by EO771-derived exosomes can functionally increase metastasis. Following the 30-day conditioning of naïve mice with EO771-derived exosomes, animals received 1×10^5 EO771 cells via the tail vein. Mice injected with EO771-derived exosomes had a higher metastatic burden in the lung

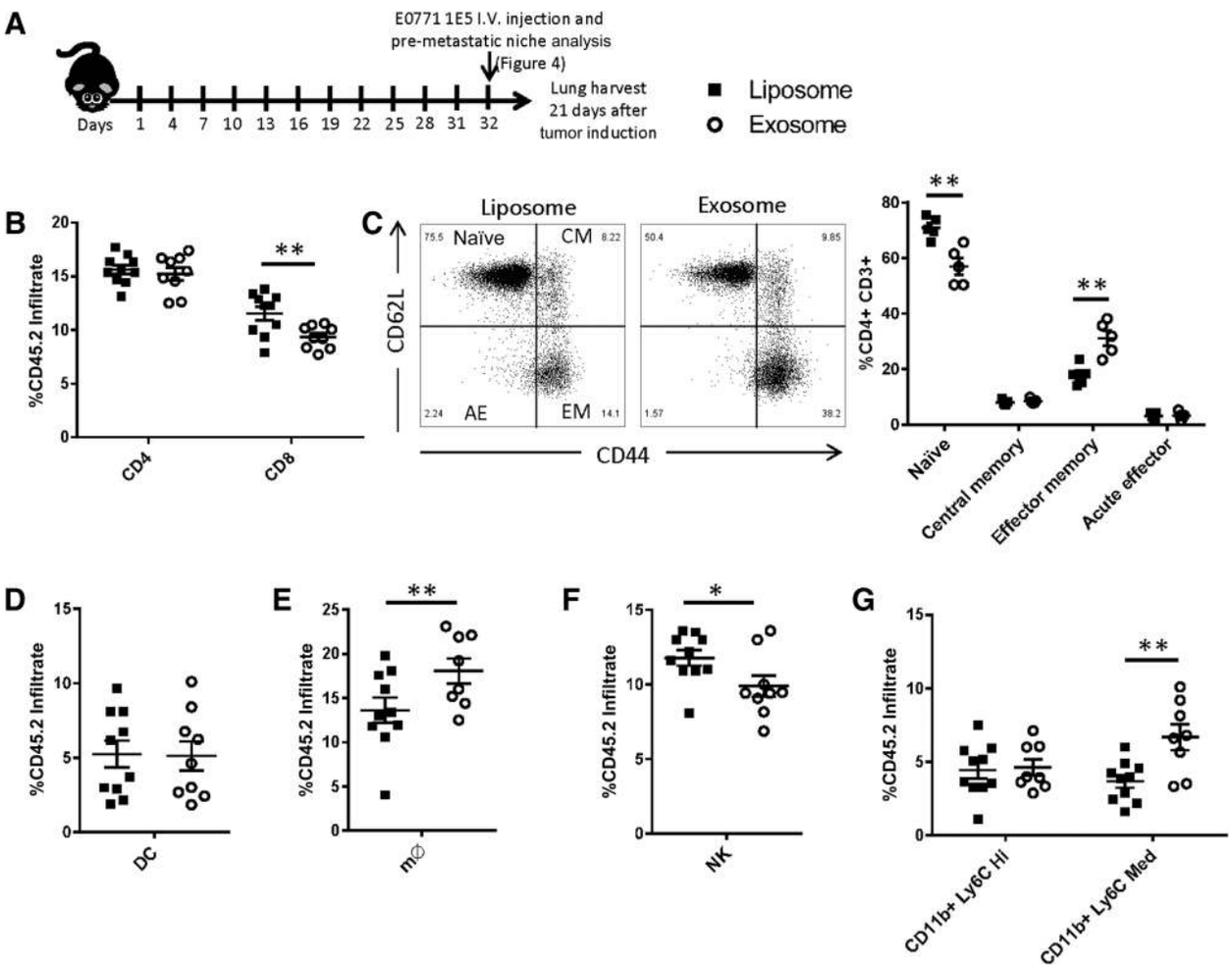

Figure 3.

Breast cancer exosomes create an immunosuppressive premetastatic niche in the lung. **A,** C57BL/6 mice received 10 μg (7.8×10^{10} particles) of EO771-derived exosomes or liposomes every 3 days for 30 days (intravenous). The frequency of various immune populations in the lung was quantified by flow cytometry at endpoint. **B,** Frequency of CD4 ($CD3^{+}/CD4^{+}$) and CD8 T cells ($CD3^{+}/CD8^{+}$) in the lung. **C,** Representative flow-cytometric plots of naïve ($CD44^{low}/CD62L^{high}$), central memory (CM; $CD44^{high}/CD62L^{high}$), effector memory (EM; $CD44^{high}/CD62L^{low}$), and acute effector $CD4^{+}$ T cells (AE; $CD44^{low}/CD62L^{low}$; left). These subpopulations of $CD4^{+}$ T cells were quantified in the lung (right). Frequency of DCs ($CD11C^{+}/MHCII^{+}$; **D**), macrophages (mø; $CD11b^{+}/F4/80^{+}$; **E**), NK cells ($NK1.1^{+}/CD3^{-}$; **F**), and $CD11b^{+}/Ly6C^{med}$ granulocytic MDSCs and $CD11b^{+}/Ly6C^{high}$ monocytic MDSCs (**G**). Results are presented as mean ± SEM ($n = 5$–10 animals/group) and analyzed by two-tailed Mann–Whitney *U* tests and the Holm–Sidak multiple testing correction method; *, $P < 0.05$; **, $P < 0.01$.

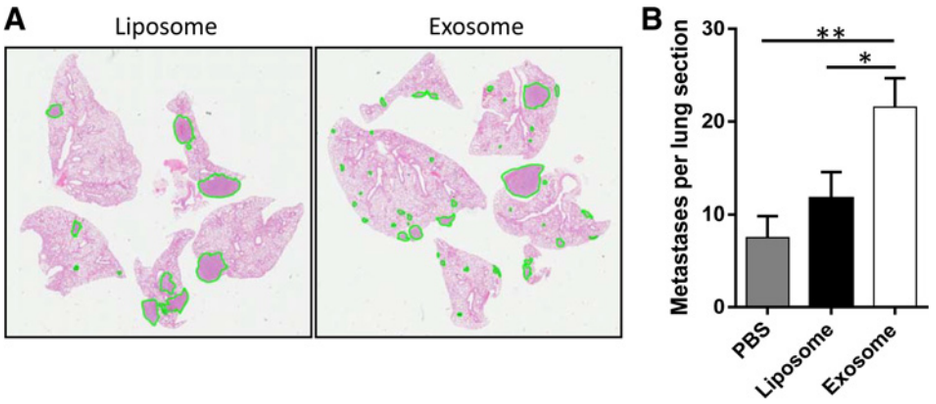

Figure 4.

Breast cancer exosomes promote metastatic colonization in the lung. C57BL/6 mice received 10 μg (7.8×10^{10} particles) of EO771-derived exosomes, liposomes, or PBS every 3 days for 30 days (intravenous). After exosome conditioning, mice received 1×10^5 EO771 cells and metastatic burden in the lung assessed 21 days later. **A,** Representative lung sections (hematoxylin and eosin) identifying metastases (circled in green). **B,** Number of metastases per lung section (two sections per lung analyzed). Results are presented as mean ± SEM ($n = 5$ animals/group) and analyzed by ANOVA. *, $P < 0.05$; **, $P < 0.01$.

(measured by histology) compared with liposome-treated and PBS control mice (Fig. 4).

Exosomes from highly metastatic breast cancer cells are required to promote metastasis

Given that breast cancer exosomes seem to create a premetastatic niche capable of promoting metastatic outgrowth, we next examined if this effect was restricted only to highly metastatic breast cancer cells. For this approach, we again conditioned naïve animals with exosomes derived this time from highly metastatic 4T1 and nonmetastatic 67NR isogenic breast cancer cells every 3 days for 30 days (Fig. 5A). Liposome-treated animals served as the control cohort. We first examined changes in T-cell, NK cell, and MDSC frequency in the lung and liver as these tissues displayed highest accumulation of systemically injected 4T1- and 67NR-derived exosomes (Fig. 5B and C). In the liver, 4T1 exosomes significantly increased the frequency of MDSCs ($CD11b^+/Gr1^+$) overall compared with both 67NR exosomes and liposome-treated groups (Fig. 5B). However, when we examined the particular MDSC subsets in the liver, we found 4T1 exosomes specifically increased the frequency of $CD11b^+/Ly6C^{high}/Ly6G^-$ cells (mMDSCs), accompanied by decreased NK cells compared with liposomes (Fig. 5B). In the lung, animals treated with 67NR-derived exosomes showed a reduced frequency of $CD11b^+/Gr1^+$ cells, but increased NK cells compared with both 4T1 exosomes- and liposome-treated animals (Fig. 5C). No change in CD4 and CD8 T-cell frequency was observed in both organs after exosome conditioning (Fig. 5B and C). Overall, the data suggest that exosomes from highly metastatic 4T1 cells are more capable than nonmetastatic 67NR exosomes at inducing MDSC recruitment.

We next examined if premetastatic niche development is exclusive to exosomes derived from cancer cells with high metastatic potential. Following the conditioning of naïve mice with 4T1- and 67NR-derived exosomes for 30 days, animals received 2.5×10^5 4T1-luciferase cells via the tail vein. Mice injected with 4T1-derived exosomes had a higher metastatic burden in both the lung (Fig. 6A) and liver (Fig. 6B) compared with 67NR exosomes, liposome-treated, and PBS control mice. This suggests that exosomes from highly metastatic breast cancer cells are required to initiate a premetastatic niche capable of promoting metastasis.

Impact of breast cancer–derived exosomes on T-cell and NK-cell functions

Given changes in the frequencies of NK cells and T cells in lungs conditioned with exosomes, we next wanted to determine if breast cancer–derived exosomes can affect these cells directly. We isolated T cells and NK cells from naïve mice and exposed them to EO771 exosomes *in vitro*. Breast cancer EO771 exosomes were capable of suppressing proliferation of both CD8 and CD4 T-cells in a dose-dependent manner (Fig. 7A and B). Flow-cytometric analysis indicated that T-cell apoptosis may be one reason for the observed reduction in CD8 and, to a lesser extent, CD4 T-cell proliferation (Supplementary Fig. S8A). This was a tumor-exosome–specific effect as liposome vesicles did not suppress T-cell proliferation (Supplementary Fig. S8B–S8C). Furthermore, the cytotoxic activity of NK cells against target tumor cells was reduced after exposure to breast cancer–derived exosomes (Fig. 7C). Together, these data demonstrate a direct effect of breast cancer–derived exosomes on the proliferative and anticancer capacities of T and NK cells.

Discussion

Metastatic spread of tumor cells to distant sites is the most common cause of cancer-related death (35). While primary tumor cells can directly release cytokines and growth factors to recruit bone marrow–derived cells to prime secondary sites for metastatic growth, we show that tumor-secreted exosomes also play a critical role. The present study uses a comprehensive *in vivo* imaging approach to describe the tissue-specific effects of exosomes from highly metastatic breast cancer cells on immune composition, and its ability to establish a premetastatic niche capable of increasing metastatic colonization.

In this study, fluorescent-tagged exosomes allowed direct *in vivo* visualization to interrogate its systemic biodistribution and uptake by $CD45^+$ cells. Here, we report that exogenously administrated (intravenous) murine breast cancer exosomes distribute predominantly to the lung regardless of metastatic potential, a frequent site of breast cancer metastasis. To a much lesser extent, breast cancer exosomes can also accumulate in the spleen. Interestingly, despite the propensity of 4T1 breast cancer cells to form

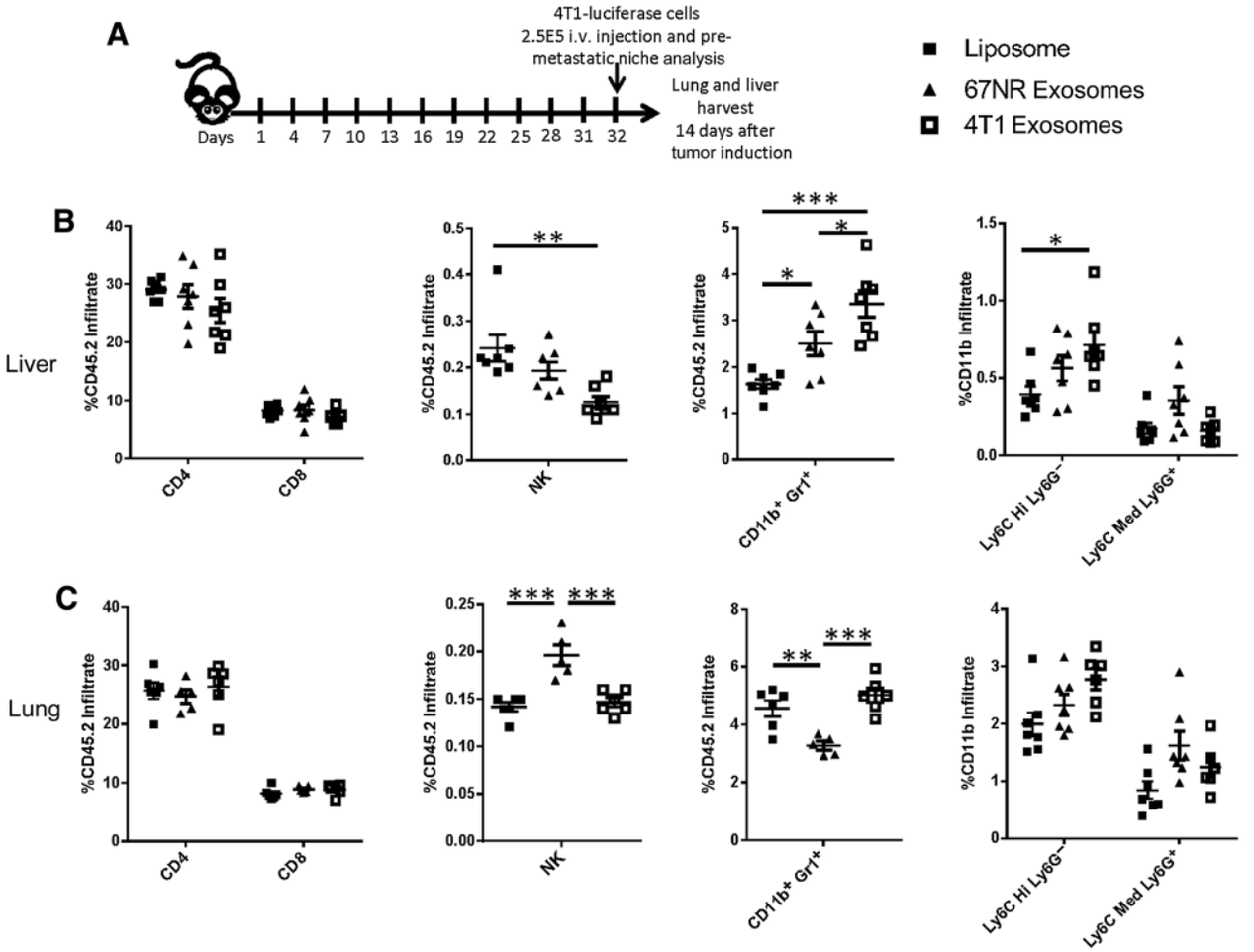

Figure 5.

Exosomes from highly metastatic 4T1 cells are more capable than nonmetastatic 67NR exosomes at inducing MDSC recruitment. **A,** BALB/c mice received 5 μg (2.9×10^{10} particles) of 4T1- or 67NR-derived exosomes every 3 days for 30 days (i.v., intravenous). Liposomes served as control. The frequency of T cells, NK cells, and MDSC subpopulations were quantified by flow cytometry at endpoint in the liver (**B**) and lung (**C**). Results are presented as mean ± SEM ($n = 6$–7 animals/group) and analyzed by ANOVA; *, $P < 0.05$; **, $P < 0.01$; ***, $P < 0.001$.

liver metastases, its secreted exosomes did not accumulate specifically in the liver compared with liposome particles, indicating that tumor exosomes may not necessarily mimic the metastatic distribution of host cells. Supporting this observation, exosomes from 67NR cells distribute significantly to both the liver and lung despite the nonmetastatic potential of host cells. Our results are in contrast to those of a recent report that showed the biodistribution of human breast cancer exosomes mimics the organotropic distribution of the cell line of origin (36). Importantly, this report showed that organotropic tumor exosomes can redirect the metastatic distribution of tumor cells (36). While the distribution of exosomes from tissue-specific breast cancer cells was shown to be consistent regardless of route of injection (i.e., retro-orbital venous sinus, the tail vein or intracardiac; ref. 36), the distribution pattern of exosomes derived from non-tumor cells lines (HEK293T epithelial cells) is highly dependent on the route of injection (37). Taken together, it is likely that the organ specificity of exosome biodistribution is driven by a multitude of factors, including cell source, injection route, tissue microenvironment, and exosome surface markers, all of which warrants further investigation to elucidate relative impact. Given the limited number of studies reporting exosome tracking (12, 36, 38, 39) and the increasing interest of using exosomes as targeted vesicles of therapeutic delivery, our study provides further evaluation and confirmation of the tissue accumulation of breast cancer exosomes. Our studies suggest that the intravenous injection of exosomes is an ideal route for *in vivo* investigations because it results in the accumulation of systemic exosomes in the lung, a frequent site of metastasis in breast cancer as well as many other cancers (e.g., colorectal, bladder, prostate, and kidney cancer). Therefore, this ideal model allows us to adequately study the consequence of exosome accumulation in premetastatic organs and speculate if its accumulation can make the lung environment more prone to metastatic tumor cell colonization.

A key hallmark and prerequisite for tumor cells to metastasize and sustain neoplastic progression is to evade immune detection and destruction (4). Commonly, this involves the concurrent co-opting of multiple immunosuppressive cell populations (40).

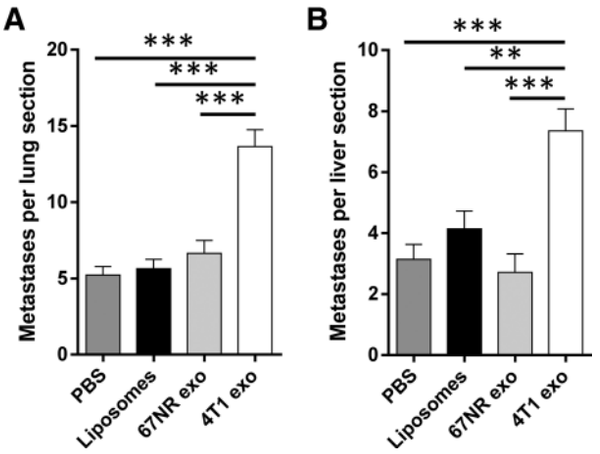

Figure 6.

Exosomes from metastatic breast cancer cells are required to initiate a premetastatic niche capable of promoting metastases. BALB/c mice received 5 μg (2.9×10^{10} particles) of 4T1- or 67NR-derived exosomes every 3 days for 30 days (intravenous). PBS and liposomes served as control treatment. After exosome conditioning, mice received 2.5×10^5 4T1-luciferase cells and metastatic burden in the lung and liver assessed 14 days later by histology. Number of metastases per lung section (**A**) and liver section (**B**). Two sections per organ were analyzed. Results are presented as mean ± SEM ($n = 7$ animals/group) and analyzed by ANOVA. **, $P < 0.01$; ***, $P < 0.001$.

Here, we report the uptake of systemic breast cancer exosomes by various immune cell lineages in organs of high exosome accumulation and the subsequent establishment of a premetastatic niche. Up to 15% of $CD45^+$ cells in the lung were shown to take up EO771 breast cancer exosomes, a majority of which were macrophages, $CD11b^+$ myeloid cells, and DCs, and to a much lesser extent, lymphocytes. This uptake pattern was also comparable between highly metastatic 4T1 and nonmetastatic 67NR isogenic breast cancer cells. It is unclear from this study if exosome uptake is cell specific. Besides immune cells, lung-tropic exosomes are known to colocalize highly with S100A4-positive fibroblasts and surfactant protein C (SPC)–positive epithelial cells in the lung (36). Target cell specificity for binding of exosomes may be determined by adhesion molecules, such as tetraspanins, galectins, and integrins, as well as major histocompatibility complex class II present on exosomes (36, 41–43). Proteomic profiling combined with selective targeting of surface proteins will be required in future studies to determine exosome markers important for specific uptake by different immune cell populations. It is most certain that the overall organ-specific response induced by tumor-derived exosomes is a collective interplay between many target cell types, including fibroblasts, immune and epithelial populations.

It is becoming increasingly clear from both proteomic and genomic profiling studies that exosomes from metastatic and benign tumors are distinctly different and reflective of the disease state (12, 31, 44–46). Our findings provide key evidence that metastatic potential is also a key determinate of exosome function in the progression of metastasis. We demonstrate that exosomes from highly metastatic breast cancer cells (4T1 and EO771 cells) can condition a favorable microenvironment that promotes metastatic colonization in the lung and liver, an effect not observed from exosomes derived from nonmetastatic cells (67NR cells) and liposome control vesicles. Specifically, the continuous accumulation and uptake of EO771 breast cancer exosomes in the lung was shown to recruit $CD11b^+/Ly6C^{med}$ gMDSCs (a subdivision of MDSCs), but decrease T-cell and NK-cell frequency, indicative of an immunosuppressive microenvironment. gMDSCs are a subpopulation of immature myeloid cells that are expanded in states of cancer and are associated with disease progression and poor prognosis, most often due to the suppression of T-cell immunity (33, 34, 47). Indeed, we showed that continuous conditioning of naïve mice with EO771-derived exosomes decreased the ratio of CD8 T-cell numbers to gMDSCs in the lung, suggesting that gMDSC recruitment by tumor exosomes may

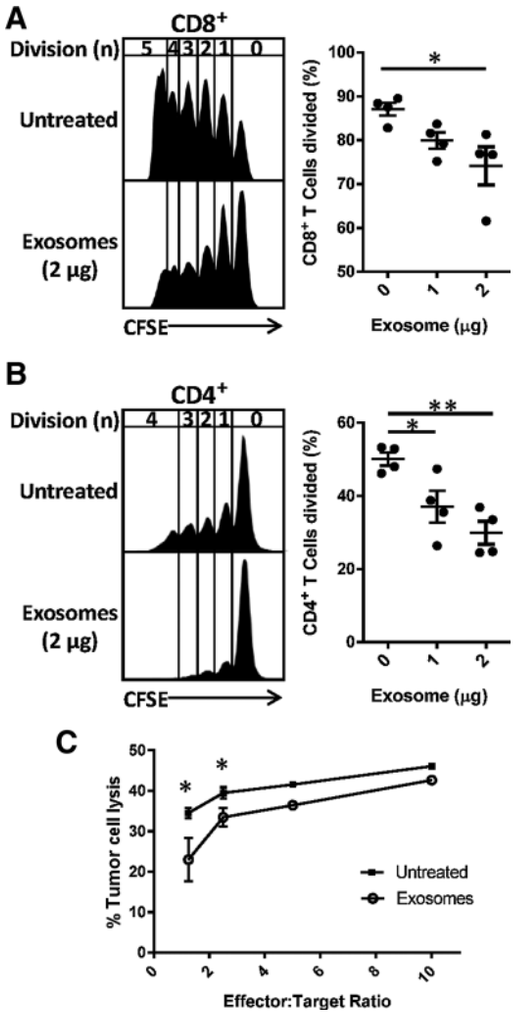

Figure 7.

Breast cancer exosomes suppress T-cell proliferation and reduces NK-cell cytotoxicity. T cells and NK cells isolated from naïve mice were exposed to EO771-derived exosomes or PBS (untreated) *in vitro*. Representative flow-cytometric histograms (left) and percentage of divided $CD8^+/CFSE^+$ T cells (right; **A**) and $CD4^+/CFSE^+$ T-cells (**B**). **C,** ^{51}Cr release cytotoxicity assay for percent lysis of target tumor cells by effector NK cells at indicated effector-to-target ratios ($n = 3$ independent experiments in triplicate). Results are presented as mean ± SEM and analyzed by ANOVA. *, $P < 0.05$; **, $P < 0.01$.

additionally regulate T cells. Furthermore, the frequency of MDSCs, as defined by the $CD11b^{+}/Gr1^{+}$ cells in a 4T1/BALB/c model (48), was also increased in the liver and lung following conditioning of naïve mice with exosomes from highly metastatic 4T1 cells. However, T-cell frequency in these organs remained unchanged. Several possible mechanisms for MDSC differentiation and recruitment by tumor-derived exosomes have been postulated by previous studies (17, 49–51). For example, exosomal PGE2 and TGF-beta secreted by breast cancer cells were reported to promote the differentiation of bone marrow myeloid cells to proinflammatory MDSCs (17). Others reported a pivotal role for Hsp72 and MyD88–Toll-like receptor (TLR) signaling in tumor exosome-mediated expansion of MDSCs and tumor progression (49, 50). Furthermore, exosomes derived from human colorectal and melanoma cells can impair the differentiation of peripheral blood monocytes to functional DCs, instead skewing them toward the phenotype of MDSCs (51). Interestingly, it was noted that 4T1 exosomes increased lung metastases despite inducing similar frequencies of MDSCs in the lung as liposome-treated controls. This suggests that exosomes may have equally important roles in MDSC accumulation, function regulation (e.g., gMDSC vs. mMDSC and cytokine secretion), and interplay with other immune cells (e.g., regulatory T cells) to promote metastatic outgrowth in premetastatic organs. Future studies to examine functional and gene expression consequences in MDSCs after exposure to tumor exosomes would be of interest to understand its overall contribution to premetastatic niche development.

Furthermore, continuous conditioning of the lung with EO771 breast cancer exosomes was shown to increase differentiation of naïve T cells ($CD44l^{ow}CD62L^{hi}$) to effector T cells ($CD44^{hi}CD62^{low}$), a phenotype observed in other tumor microenvironments where T cells then proceed to terminal differentiation into "exhausted" T cells (52). Exhausted T cells are no longer functional and express high levels of immune inhibitory receptors, leading to cancer immune evasion (52). In line with our *in vivo* observation, the immunosuppressive nature of breast cancer exosomes was confirmed *in vitro* where it inhibited T-cell proliferation by initiating cell apoptosis and NK-cell cytotoxicity. It is possible that breast cancer exosomes are directly inducing apoptosis in activated T cells by the transfer of the death ligands FasL and TRAIL, a mechanism demonstrated in exosomes derived from other cancer types (16, 53, 54). Future studies to extensively characterize other immune cells types that demonstrated high exosome uptake, such as macrophages and DCs, would be important. Additionally, systemically injected breast cancer exosomes may have additionally effects in organs other than the liver and lung (e.g., lymphoid organs) that contribute to tumor progression and warrant further investigation.

Overall, understanding the role and function of tumor-derived exosomes has important implications not just for the understanding of metastatic progression in breast cancer, but also in limiting the efficacy of current clinical and preclinical immunotherapeutics, which is currently not taken into consideration. Given that tumor-derived exosomes can target immune cells to alter its composition and induce an immunosuppressive tissue environment, they present potential targets of novel anticancer therapeutics in breast cancer. It may therefore be beneficial to selectively deplete tumor-specific exosomes in circulation by extracorporeal hemofiltration approaches (55), or develop inhibitors that interfere with tumor-exosome uptake. Future studies will focus on detailed proteomic and RNA profiling of breast cancer–derived exosomes to identify exosomal content responsible for driving immune regulation.

Disclosure of Potential Conflicts of Interest

No potential conflicts of interest were disclosed.

Authors' Contributions

Conception and design: S.W. Wen, B.S. Parker, A. Möller
Development of methodology: S.W. Wen, J. Sceneay, S. Krumeich, R.J. Lobb, K.N. Wong, S. Ellis
Acquisition of data (provided animals, acquired and managed patients, provided facilities, etc.): S.W. Wen, L.G. Lima, C.S.F. Wong, M. Becker, S. Krumeich, R.J. Lobb, K.N. Wong, S. Ellis
Analysis and interpretation of data (e.g., statistical analysis, biostatistics, computational analysis): S.W. Wen, J. Sceneay, L.G. Lima, M. Becker, S. Krumeich, S. Ellis, A. Möller
Writing, review, and/or revision of the manuscript: S.W. Wen, J. Sceneay, L.G. Lima, C.S.F. Wong, S. Krumeich, K.N. Wong, S. Ellis, B.S. Parker, A. Möller
Administrative, technical, or material support (i.e., reporting or organizing data, constructing databases): S.W. Wen, C.S.F. Wong, M. Becker, S. Krumeich
Study supervision: S.W. Wen, B.S. Parker, A. Möller
Other (generated data by performing experiments crucial to the paper): V. Castillo

Acknowledgments

We thank Stuart Olver from the Bone Marrow Transplantation at QIMR Berghofer for his assistance with the ^{51}Cr release cytotoxicity assay.

Grant Support

This work was supported by grants of the National Health and Medical Research Council Australia to A. Möller (APP1068510), Cancer Council Queensland to A. Möller (APP1045620), Rio-Tinto-Ride-To-Conquer-Cancer to A. Möller (6156), a National Breast Cancer Foundation (Australia) fellowship and grant, both to A. Möller (ECF-11-09, NC-13-26), and an ARC Fellowship to B.S. Parker (FT130100671).

The costs of publication of this article were defrayed in part by the payment of page charges. This article must therefore be hereby marked *advertisement* in accordance with 18 U.S.C. Section 1734 solely to indicate this fact.

Received March 30, 2016; revised September 9, 2016; accepted September 26, 2016; published OnlineFirst October 19, 2016.

References

1. Siegel R, Ma J, Zou Z, Jemal A. Cancer statistics, 2014. CA Cancer J Clin 2014;64:9–29.
2. Sledge GW, Mamounas EP, Hortobagyi GN, Burstein HJ, Goodwin PJ, Wolff AC. Past, present, and future challenges in breast cancer treatment. J Clin Oncol 2014;32:1979–86.
3. McAllister SS, Weinberg RA. The tumour-induced systemic environment as a critical regulator of cancer progression and metastasis. Nat Cell Biol 2014;16:717–27.
4. Hanahan D, Weinberg RA. Hallmarks of cancer: the next generation. Cell 2011;144:646–74.
5. Thery C, Zitvogel L, Amigorena S. Exosomes: composition, biogenesis and function. Nat Rev Immunol 2002;2:569–79.
6. Vlassov AV, Magdaleno S, Setterquist R, Conrad R. Exosomes: current knowledge of their composition, biological functions, and diagnostic and therapeutic potentials. Biochim Biophys Acta 2012;1820:940–8.

7. Al-Nedawi K, Meehan B, Kerbel RS, Allison AC, Rak J. Endothelial expression of autocrine VEGF upon the uptake of tumor-derived microvesicles containing oncogenic EGFR. Proc Natl Acad Sci U S A 2009; 106:3794–9.
8. Al-Nedawi K, Meehan B, Micallef J, Lhotak V, May L, Guha A, et al. Intercellular transfer of the oncogenic receptor EGFRvIII by microvesicles derived from tumour cells. Nat Cell Biol 2008;10: 619–24.
9. Ciravolo V, Huber V, Ghedini GC, Venturelli E, Bianchi F, Campiglio M, et al. Potential role of HER2-overexpressing exosomes in countering trastuzumab-based therapy. J Cell Physiol 2012;227:658–67.
10. Kucharzewska P, Christianson HC, Welch JE, Svensson KJ, Fredlund E, Ringner M, et al. Exosomes reflect the hypoxic status of glioma cells and mediate hypoxia-dependent activation of vascular cells during tumor development. Proc Natl Acad Sci U S A 2013;110: 7312–7.
11. Wen S, Lobb R, Möller A. Exosomes in cancer metastasis: novel targets for diagnosis and therapy? Cancer Forum, Cancer Council Australia 2014; 38:116–9.
12. Costa-Silva B, Aiello NM, Ocean AJ, Singh S, Zhang H, Thakur BK, et al. Pancreatic cancer exosomes initiate pre-metastatic niche formation in the liver. Nat Cell Biol 2015;17:816–26.
13. Sceneay J, Parker BS, Smyth MJ, Moller A. Hypoxia-driven immunosuppression contributes to the pre-metastatic niche. Oncoimmunology 2013;2:e22355.
14. Sceneay J, Smyth MJ, Moller A. The pre-metastatic niche: finding common ground. Cancer Metastasis Rev 2013;32:449–64.
15. Peinado H, Aleckovic M, Lavotshkin S, Matei I, Costa-Silva B, Moreno-Bueno G, et al. Melanoma exosomes educate bone marrow progenitor cells toward a pro-metastatic phenotype through MET. Nat Med 2012;18: 883–91.
16. Taylor DD, Gercel-Taylor C, Lyons KS, Stanson J, Whiteside TL. T-cell apoptosis and suppression of T-cell receptor/CD3-zeta by Fas ligand-containing membrane vesicles shed from ovarian tumors. Clin Cancer Res 2003;9:5113–9.
17. Xiang X, Poliakov A, Liu C, Liu Y, Deng ZB, Wang J, et al. Induction of myeloid-derived suppressor cells by tumor exosomes. Int J Cancer 2009;124:2621–33.
18. Bidwell BN, Slaney CY, Withana NP, Forster S, Cao Y, Loi S, et al. Silencing of Irf7 pathways in breast cancer cells promotes bone metastasis through immune escape. Nat Med 2012;18:1224–31.
19. Casey AE, Laster WRJr., Ross GL. Sustained enhanced growth of carcinoma EO771 in C57 black mice. Exp Biol Med 1951;77:358–62.
20. Moller A, House CM, Wong CS, Scanlon DB, Liu MC, Ronai Z, et al. Inhibition of Siah ubiquitin ligase function. Oncogene 2009;28: 289–96.
21. Pulaski BA, Ostrand-Rosenberg S. Mouse 4T1 breast tumor model. Current protocols in immunology/edited by John E Coligan [et al] 2001;Chapter 20:Unit202.
22. Sceneay J, Liu MC, Chen A, Wong CS, Bowtell DD, Moller A. The antioxidant N-acetylcysteine prevents HIF-1 stabilization under hypoxia in vitro but does not affect tumorigenesis in multiple breast cancer models in vivo. PloS ONE 2013;8:e66388.
23. Lobb RJ, Becker M, Wen SW, Wong CS, Wiegmans AP, Leimgruber A, et al. Optimized exosome isolation protocol for cell culture supernatant and human plasma. J Extracellular Vesicles 2015;4:27031.
24. Hoshino A, Costa-Silva B, Shen TL, Rodrigues G, Hashimoto A, Tesic Mark M, et al. Tumour exosome integrins determine organotropic metastasis. Nature 2015;527:329–35.
25. Mathivanan S, Lim JW, Tauro BJ, Ji H, Moritz RL, Simpson RJ. Proteomics analysis of A33 immunoaffinity-purified exosomes released from the human colon tumor cell line LIM1215 reveals a tissue-specific protein signature. Mol Cell Proteomics 2010;9:197–208.
26. de Vrij J, Maas SL, van Nispen M, Sena-Esteves M, Limpens RW, Koster AJ, et al. Quantification of nanosized extracellular membrane vesicles with scanning ion occlusion sensing. Nanomedicine 2013; 8:1443–58.
27. Roberts GS, Kozak D, Anderson W, Broom MF, Vogel R, Trau M. Tunable nano/micropores for particle detection and discrimination: scanning ion occlusion spectroscopy. Small 2010;6:2653–8.
28. Lyons AB, Parish CR. Determination of lymphocyte division by flow cytometry. J Immunol Methods 1994;171:131–7.
29. Chan CJ, Andrews DM, McLaughlin NM, Yagita H, Gilfillan S, Colonna M, et al. DNAM-1/CD155 interactions promote cytokine and NK cell-mediated suppression of poorly immunogenic melanoma metastases. J Immunol 2010;184:902–11.
30. Sceneay J, Chow MT, Chen A, Halse HM, Wong CS, Andrews DM, et al. Primary tumor hypoxia recruits CD11b+/Ly6Cmed/Ly6G+ immune suppressor cells and compromises NK cell cytotoxicity in the premetastatic niche. Cancer Res 2012;72:3906–11.
31. Logozzi M, De Milito A, Lugini L, Borghi M, Calabro L, Spada M, et al. High levels of exosomes expressing CD63 and caveolin-1 in plasma of melanoma patients. PloS One 2009;4:e5219.
32. Taylor DD, Lyons KS, Gercel-Taylor C. Shed membrane fragment-associated markers for endometrial and ovarian cancers. Gynecol Oncol 2002;84:443–8.
33. Raber PL, Thevenot P, Sierra R, Wyczechowska D, Halle D, Ramirez ME, et al. Subpopulations of myeloid-derived suppressor cells impair T cell responses through independent nitric oxide-related pathways. Int J Cancer 2014;134:2853–64.
34. Talmadge JE, Gabrilovich DI. History of myeloid-derived suppressor cells. Nat Rev Cancer 2013;13:739–52.
35. Gupta GP, Massague J. Cancer metastasis: building a framework. Cell 2006;127:679–95.
36. Hoshino A, Costa-Silva B, Shen TL, Rodrigues G, Hashimoto A, Tesic Mark M, et al. Tumour exosome integrins determine organotropic metastasis. Nature 2015;527:329–35.
37. Wiklander OP, Nordin JZ, O'Loughlin A, Gustafsson Y, Corso G, Mager I, et al. Extracellular vesicle in vivo biodistribution is determined by cell source, route of administration and targeting. J Extracellular Vesicles 2015;4:26316.
38. Sun D, Zhuang X, Xiang X, Liu Y, Zhang S, Liu C, et al. A novel nanoparticle drug delivery system: the anti-inflammatory activity of curcumin is enhanced when encapsulated in exosomes. Mol Ther 2010;18:1606–14.
39. Zhuang X, Xiang X, Grizzle W, Sun D, Zhang S, Axtell RC, et al. Treatment of brain inflammatory diseases by delivering exosome encapsulated anti-inflammatory drugs from the nasal region to the brain. Mol Ther 2011; 19:1769–79.
40. Kim R, Emi M, Tanabe K. Cancer immunoediting from immune surveillance to immune escape. Immunology 2007;121:1–14.
41. Mallegol J, Van Niel G, Lebreton C, Lepelletier Y, Candalh C, Dugave C, et al. T84-intestinal epithelial exosomes bear MHC class II/peptide complexes potentiating antigen presentation by dendritic cells. Gastroenterology 2007;132:1866–76.
42. Rana S, Yue S, Stadel D, Zoller M. Toward tailored exosomes: the exosomal tetraspanin web contributes to target cell selection. Int J Biochem Cell Biol 2012;44:1574–84.
43. Segura E, Guerin C, Hogg N, Amigorena S, Thery C. CD8+ dendritic cells use LFA-1 to capture MHC-peptide complexes from exosomes in vivo. J Immunol 2007;179:1489–96.
44. Isin M, Uysaler E, Ozgur E, Koseoglu H, Sanli O, Yucel OB, et al. Exosomal lncRNA-p21 levels may help to distinguish prostate cancer from benign disease. Front Genet 2015;6:168.
45. Skog J, Wurdinger T, van Rijn S, Meijer DH, Gainche L, Sena-Esteves M, et al. Glioblastoma microvesicles transport RNA and proteins that promote tumour growth and provide diagnostic biomarkers. Nat Cell Biol 2008;10:1470–6.
46. Taylor DD, Gercel-Taylor C. MicroRNA signatures of tumor-derived exosomes as diagnostic biomarkers of ovarian cancer. Gynecol Oncol 2008;110:13–21.
47. Montero AJ, Diaz-Montero CM, Kyriakopoulos CE, Bronte V, Mandruzzato S. Myeloid-derived suppressor cells in cancer patients: a clinical perspective. J Immunother 2012;35:107–15.
48. Chafe SC, Lou Y, Sceneay J, Vallejo M, Hamilton MJ, McDonald PC, et al. Carbonic anhydrase IX promotes myeloid-derived suppressor cell mobilization and establishment of a metastatic niche by stimulating G-CSF production. Cancer Res 2015;75:996–1008.
49. Chalmin F, Ladoire S, Mignot G, Vincent J, Bruchard M, Remy-Martin JP, et al. Membrane-associated Hsp72 from tumor-derived exosomes mediates STAT3-dependent immunosuppressive function of mouse and human myeloid-derived suppressor cells. J Clin Invest 2010;120:457–71.

50. Liu Y, Xiang X, Zhuang X, Zhang S, Liu C, Cheng Z, et al. Contribution of MyD88 to the tumor exosome-mediated induction of myeloid derived suppressor cells. Am J Pathol 2010;176:2490–9.
51. Valenti R, Huber V, Filipazzi P, Pilla L, Sovena G, Villa A, et al. Human tumor-released microvesicles promote the differentiation of myeloid cells with transforming growth factor-beta-mediated suppressive activity on T lymphocytes. Cancer Res 2006;66:9290–8.
52. Jiang Y, Li Y, Zhu B. T-cell exhaustion in the tumor microenvironment. Cell Death Dis 2015;6:e1792.
53. Andreola G, Rivoltini L, Castelli C, Huber V, Perego P, Deho P, et al. Induction of lymphocyte apoptosis by tumor cell secretion of FasL-bearing microvesicles. J Exp Med 2002;195:1303–16.
54. Wieckowski EU, Visus C, Szajnik M, Szczepanski MJ, Storkus WJ, Whiteside TL. Tumor-derived microvesicles promote regulatory T cell expansion and induce apoptosis in tumor-reactive activated CD8+ T lymphocytes. J Immunol 2009;183:3720–30.
55. Ichim TE, Zhong Z, Kaushal S, Zheng X, Ren X, Hao X, et al. Exosomes as a tumor immune escape mechanism: possible therapeutic implications. J Translat Med 2008;6:37.